ARTICLE

Response Characteristics of Strain Sensors Based on Closely Spaced Nanocluster Films with Controlled Coverage†

Fei Liu[a*], Wei Shao[a,b], Gan Xu[a], Ling Yuan[a]

a. Department of Materials Science and Engineering, Nanjing University, Nanjing 210093, China
b. Suzhou SinoRaybo Nanotechnology Co., Ltd., Suzhou 215123, China

(Dated: Received on December 29, 2018; Accepted on February 3, 2019)

Flexible strain sensor devices were fabricated by depositing Pd nanoclusters on PET membranes patterned with interdigital electrodes. The sensors responded to the deformation of the PET membranes with the conductance changes of the nanocluster films and were characterized by both high gauge factor and wide detection range. The response characteristics of the strain sensors were found to depend strongly on the nanocluster coverage, which was attributed to the percolative nature of the electron transport in the closely spaced nanocluster arrays. By controlling the nanocluster deposition process, a strain sensor composed of nanocluster arrays with a coverage close to the effective percolation threshold was fabricated. The sensor device showed a linear response with a stable gauge factor of 55 for the applied strains from the lower detection limit up to 0.3%. At higher applied strains, a gauge factor as high as 200 was shown. The nanocluster films also demonstrated the ability to response to large deformations up to 8% applied strain, with an extremely high gauge factor of 3500.

Key words: Nanocluster film, Electron transport, Strain sensor, Coverage, Percolation

I. INTRODUCTION

The measurement of strain is important in numerous applications in science, engineering and medicine. Strain sensors are one of the most widely used transducers offered in a wide variety of patterns for scientific, industrial and experimental stress analysis. Traditional metallic strain gauges have been widely used. The discovery of the piezoresistive effect in silicon generated significant interest in semiconductor strain sensing. Despite their excellent features, these conventional strain sensors show some limitations. Metallic foil strain gauges are more or less flexible but their gauge factors are typically low [1]. Semiconductor strain gauges can have a much larger gauge factor as high as 100 but are fragile with a high temperature coefficient [2].

More recently, the development of structural health monitoring systems [3, 4], wearable devices [5, 6], electronic skin [7, 8] as well as healthcare and medical diagnosis devices [9, 10] has drawn tremendous attention towards the development of new flexible strain sensors characterized by high sensitivity, wide detection range, easy signal processing, low cost and simple manufacturing process. Researches have been focusing on driving device designs to the nanoscale. Many types of nanostructure based strain sensing materials have been studied, including nanowires [11, 12], nanotubes [13–15], graphene [16–18], nanoparticle films [19–21], as well as nano-polysilicon thin film transistors [22]. Excellent strain sensing characteristics have been demonstrated by them due to their novel microstructures.

Quantum conductance of closely spaced metal nanocluster arrays fabricated on the flexible substrate surface has recently been investigated for the design of strain sensors [21]. The sensing mechanism of such strain sensors is based on the deformation-dependent conductive percolation morphology over the nanocluster arrays. The current transport in such arrays is dominated by the thermally activated hopping of electrons across the barriers present in between neighboring nanoclusters. A small deformation of the flexible substrate induces a change on the interspacing of the nanoclusters, enabling more or less conductive percolation pathways, leading to a change of the electron conductance. Compared to the conventional strain sensors utilizing the piezoresistance property of bulk metal or silicon, the flexible strain sensors based on the nanocluster arrays exhibit high strain tolerance, high sensitivity, and low power consumption. Our previous study [23] showed that the quantum conductance characteristics of the closely spaced nanocluster arrays depended strongly on the nanocluster coverage. In this work, we study the influence of the nanocluster coverage on the response characteristics of the nanocluster strain sensors, which is crucial for the sensor applications. We show that by optimizing the nanocluster coverage, high sensitivity

†Part of the special issue for "the 19th International Symposium on Small Particles and Inorganic Clusters"
*Author to whom correspondence should be addressed. E-mail: feiliu1987@nju.edu.cn

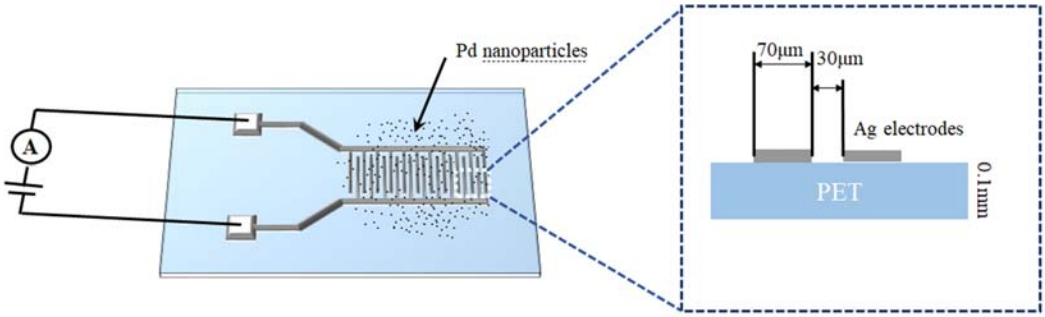

FIG. 1 Schematic illustration of the nanocluster film based strain sensor.

and wide working range can be realized.

II. EXPERIMENTS

We fabricated the strain sensors by gas phase depositing Pd nanocluster films with controlled coverage on polyethylene terephthalate (PET) membranes decorated with silver interdigital electrodes. PET is an effective substrate for flexible sensors. Generally nanoclusters of various metals can be used in the quantum conductance based strain sensors. In this work, Pd nanoclusters were used due to their chemical stability and good adhesion to substrates. In fact, Pd nanoclusters have been well used in various sensors [23–25]. A schematic view of the sensor fabrication is shown in FIG. 1. Silver interdigital electrodes were patterned onto the PET membranes by shadow mask evaporation in high vacuum. The thickness of the PET membranes was 0.1 mm. The width of the interdigital electrodes was 70 μm, with a 30 μm electrode separation. The whole electrodes covered an area of about 7.5 mm×9.0 mm. The thickness of the silver electrodes was about 100 nm.

Nanocluster deposition was performed in a high vacuum chamber equipped with a magnetron plasma gas aggregation cluster source [23]. Atoms were sputtered from the Pd target and Pd nanoclusters were formed through the aggregation process in the argon gas. A stable argon gas flow (100 sccm) was introduced into the liquid nitrogen cooled aggregation tube to maintain a constant carrier gas pressure of about 80 Pa for cluster growth. The nanocluster size was controlled by the carrier gas pressure. The nanoclusters were swept by the gas stream into a high vacuum chamber through a nozzle and deposited on the PET membrane surface. The deposition rate was monitored by a quartz crystal microbalance and controlled to be about 0.3 Å/s by a discharge power of 30 W. The deposited nanoclusters distributed on the PET surface with an area of about 15 mm in diameter so that the whole interdigital electrodes were well covered by the nanoclusters.

During the deposition, the conductance of the nanocluster arrays that covered the interdigital electrodes was measured *in situ* with a digital multimeter (Keithley 2601) under a bias of 1 V. The deposition was stopped at a predetermined conductance value by operating a shutter, and a nanocluster film with a certain coverage was then fabricated. There was a one-to-one correspondence between each coverage and each conductance.

The morphology of the Pd nanocluster films was characterized with a transmission electron microscopy (TEM, FEI TECNAI F20s TWIN). For TEM imaging, Pd nanoclusters were deposited on the surface of amorphous carbon film supported by copper grid.

The conductance response characteristics of the strain sensors were evaluated by subjecting them either to a series of bending cycles or to a series of pull-and-release cycles. In both cases, the deformation was driven with a micrometer. The strain (ε) was calculated from the deformation according to the geometry of the measurement configuration. Generally the pull-and-release test could generate much larger deformation than the bending test, so that it was mainly used for large strain measurement. The conductance changes induced by the applied strains were measured by recording the current in the samples with a digital source meter (Keithley 2400) by applying a constant bias voltage of 1 V to the interdigital electrodes.

III. RESULTS AND DISCUSSION

FIG. 2 shows the TEM images of Pd nanoclusters prepared with different deposition time at a controlled deposition rate of 0.3 Å/s. As shown in the figure, the Pd nanoclusters distributed on the substrate surface randomly. The mean diameter of the nanoclusters was 8.3 nm and did not change with the deposition time. Previous studies [26, 27] showed that small nanoclusters of noble metals, such as Ag nanoclusters, had high mobility on the substrate subsurface, which induced significant diffusion and coalescence of nanoclus-

DOI:10.1063/1674-0068/cjcp1812296

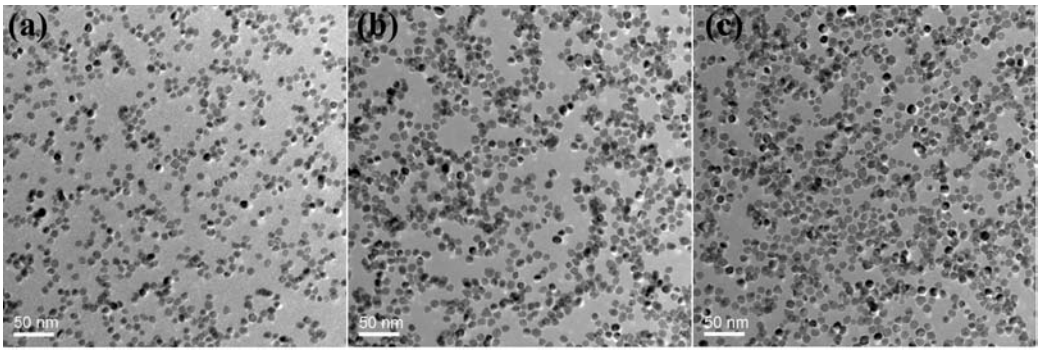

FIG. 2 TEM images for 3 samples of Pd nanocluster films with deposition time of (a) 430 s, (b) 640 s, (c) 710 s.

ters after they were deposited on the surface. Therefore, the size of the nanoclusters increased with the deposition time for a dense array of nanoclusters produced by gas phase cluster beam deposition. However, for Pd nanoclusters our results showed that there was no direct correlation between their size and the deposition time, which indicated that diffusive growth was not significant for Pd nanoclusters on the surface. It provides a simple way to modify the nanocluster number density by controlling the deposition time for different time of 430, 640, 710 s. The surface coverage of the nanoclusters in FIG. 2 (a)−(c) was measured to be 26%, 38% and 43%, respectively. With the increase of the nanocluster coverage, more and more percolation paths for electron conduction were formed between the electrodes, resulted in an increase of the conductance of the nanocluster film. We define the conductance of the unstrained strain sensor as the base conductance G_0. Corresponding to the above nanocluster coverage, the base conductance of the fabricated strain sensors was 0.21, 0.38, and 0.66 μS, respectively.

FIG. 3 shows the conductance response curve (conductance versus time diagram) measured for the specimen with a base conductance of 0.21 μS, which represents the typical responses of all the samples. The curve gives the real time electrical responses during the stepwise bending of the nanocluster coated PET substrate. The deformation pattern is shown schematically in the inset of FIG. 3. The bending of the PET membrane induced a shrink on the surface where the nanoclusters deposited. The inter-particle distance in the nanocluster film thus decreased, which resulted in an increase on the conductance of the nanocluster arrays. In FIG. 3, each bending step generated an additional 0.04% strain on its surface. An immediate electric conductance change could always be observed. When the bending was released, the conductance could be recovered inversely.

In FIG. 4, the relative resistance changes ($\Delta R/R_0$, where $\Delta R{=}R{-}R_0$, R_0 is the resistance corresponding to the base conductance G_0) of the 3 samples with different base conductance are plotted as a function of the applied strains. To investigate the response behavior

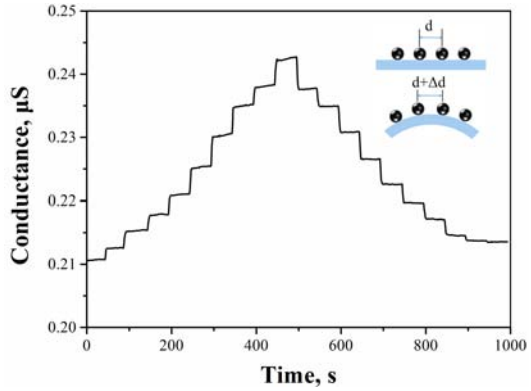

FIG. 3 Electrical conductance response curve for a strain sensor under bending deformation. The insert shows the deformation pattern of the PET membrane and the nanocluster array in the measurement.

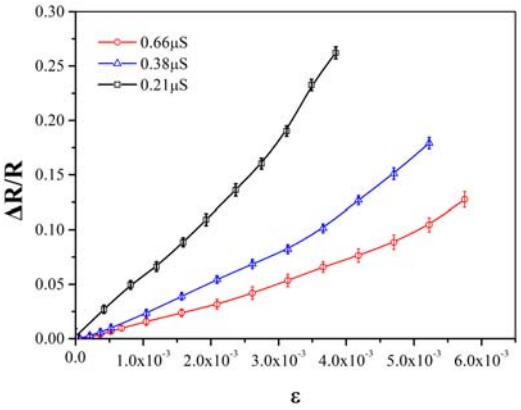

FIG. 4 Relative resistance changes as a function of the applied strain measured for the nanocluster film based strain sensors with different coverage.

under relative large strain, the strain was applied to the sensors by stretching the PET membrane surface where the nanoclusters deposited. This was realized either by bending the membrane towards the opposite side of the

DOI:10.1063/1674-0068/cjcp1812296

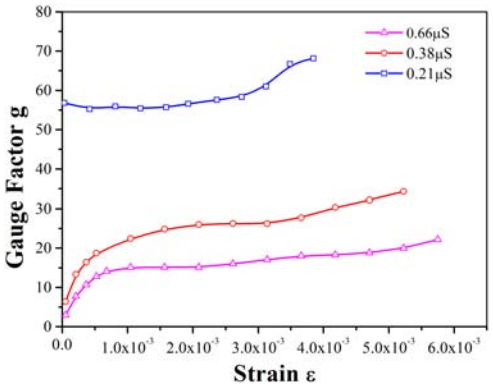

FIG. 5 Gauge factors as a function of the applied strains for the nanocluster film based strain sensors with different coverage.

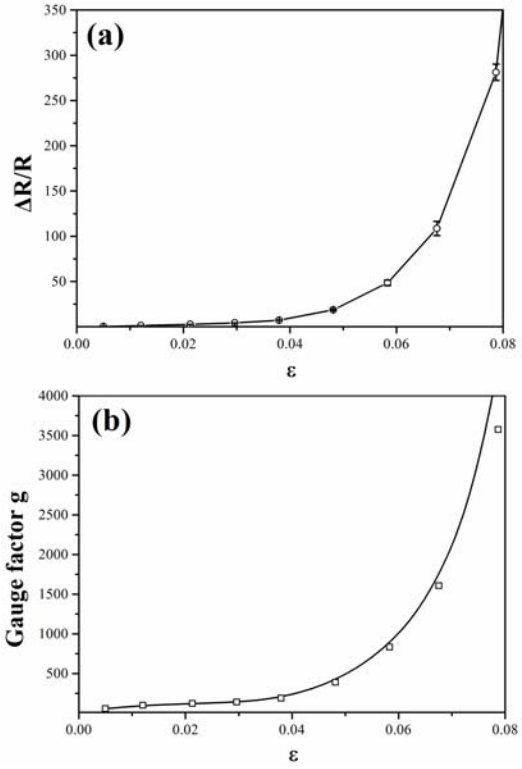

FIG. 6 Relative resistance changes (a) and gauge factors of the strain sensor under large applied strain up to 8%.

nanocluster-coated surface or by pulling the membrane linearly. It could be seen that the relative resistance change induced by the applied strain increased with the base conductance G_0 of the sensor, *i.e.*, the coverage of the nanocluster film, indicating that lower nanocluster coverage was conducive to higher sensitivity. This could be understood by considering the sensing mechanism of the closely spaced nanocluster film based sensors. The quantum conductance of the nanocluster film was directly related to the number of the electron percolation pathways it contained. There will be a sensitive dependence of the conductance on the nanocluster coverage when the latter is close to the effective percolation threshold defined by the gap size of the interdigital electrodes [28]. For nanocluster coverage far above the effective percolation threshold, the influence of the coverage change on the conductance would be much less significant. The applied strain induced a stretching on the PET membrane, which was equivalent to a decrease of the nanocluster coverage. This would generate more significant change on the quantum conductance of the nanocluster array with lower coverage, due to the loss of the electron percolation paths. Furthermore, films with lower nanocluster coverage contained less number of electron percolation pathways, so that the loss of the electron percolation paths induced by stretching, which increased the inter-particle spacing, would also generate more significant influence on the quantum conductance.

Generally, the sensitivity of a strain sensor is characterized with the gauge factor $g=(\Delta R/R_0)/\varepsilon$. In FIG. 5, the gauge factors of the nanocluster film based strain sensors with different coverage were plotted as a function of the applied strains. For the two samples with larger nanocluster coverage (G_0=0.38 and 0.66 μS), the gauge factors were low at small applied strain and increased rapidly with the increase of the strain. The low gauge factor at small strain should be attributed to the high nanocluster density that saturated the electron percolation patterns. In the moderate strain region, from 0.1% to 0.3%, all the three strain sensors hold constant gauge factors, which were about 15, 25, and 55 respectively and increased with the nanocluster coverage. For the strain sensor with the lowest nanocluster coverage (G_0=0.21 μS), the gauge factor kept high even at the lowest applied strain. The constant gauge factors enabled a linear response of the relative resistance change to the applied strains, as can be seen from FIG. 4. When the applied strain was larger than 0.3%, all the three sensors showed a further increasing on their gauge factors. This behavior should also be attributed to the effect of the nanocluster coverage. The applied strain induced a stretching on the PET membrane, which decreased the nanocluster coverage. As has been analyzed above, lower nanocluster coverage was conducive to higher sensitivity.

Detection range is another important parameter for the flexible strain sensors. To clarify the up limit of the strain that can be measured by the sensor, the strain sensor with the lowest nanocluster coverage (G_0=0.21 μS) was stretched linearly up to 8% strain. The relative resistance changes as well as the gauge factors are shown in FIG. 6. We can see that the sensor could response to the applied strains over the whole range, and the gauge factor increased with the applied strain continuously. At 8% applied strain, the gauge factor was as high as 3500. For a strain sensor fabri-

DOI:10.1063/1674-0068/cjcp1812296

cated on PET membrane, this was somewhat meaningless since the 8% strain was far above its elastic limit (∼4%). However, our result demonstrated that the conductance of the Pd nanocluster arrays could well response to such large deformations. It is possible to enlarge the detection range of such a kind of strain sensors by replacing the PET membrane with more elastic materials. Within the elastic limit, the gauge factor of the PET membrane based strain sensor could be as high as 200, which was significantly better than the typical gauge factor of semiconductor strain sensors (∼100).

IV. CONCLUSION

A flexible strain sensor device with both high gauge factor and wide detection range has been demonstrated by depositing thin films of Pd nanoclusters on PET membranes patterned with interdigital electrodes. An immediate response of the conductance of the nanocluster films to deformation of the PET membrane was shown. The response characteristics of the strain sensors was found to depend strongly on the nanocluster coverage. Devices with lower nanocluster coverage showed larger gauge factors. The coverage dependent response characteristics was attributed to the percolative nature of the electron transport in the closely spaced nanocluster arrays. The conductance was sensitively dependent on the nanocluster coverage, which could be changed by the strain applied on the substrate membrane, when the latter is close to the effective percolation threshold defined by the gap size of the interdigital electrodes. The nanocluster coverage could easily be regulated by controlling the nanocluster deposition so that an optimized strain sensor device was obtained. Linear response with a stable gauge factor of 55 was demonstrated for the applied strains from the lower detection limit of the sensor up to 0.3%. At higher strain, the gauge factor increased with the applied strains and reached 200 within the elastic limit of the PET membrane (corresponding to 4% strain). The nanocluster films also demonstrated the ability to respond to large deformations up to 8% applied strain, with an extremely high gauge factor of 3500.

V. ACKNOWLEDGEMENTS

This work was supported by the National Natural Science Foundation of China (No.11627806) and a Project funded by the Priority Academic Programme Development of Jiangsu Higher Education Institutions.

[1] M. Amjadi, A. Pichitpajongkit, S. Lee, S. Ryu, and I. Park, ACS Nano **8**, 5154 (2014).
[2] C. Farcau, H. Moreira, B. Viallet, J. Grisolia, D. Ciuculescu-Pradines, C. Amiens, and L. Ressier, J. Phys. Chem. C **115**, 14494 (2011).
[3] X. Li, C. Levy, and L. Elaadil, Nanotechnology **19**, 045501 (2008).
[4] J. Zhang, J. Liu, R. Zhuang, E. Mader, G. Heinrich, and S. Gao, Adv. Mater. **23**, 3392 (2011).
[5] S. Yao and Y. Zhu, Nanoscale **6**, 2345 (2014).
[6] X. Liao, Q. Liao, X. Yan, Q. Liang, H. Si, M. Li, H. Wu, S. Cao, and Y. Zhang, Adv. Func. Mater. **25**, 2395 (2015).
[7] C. Pang, G. Y. Lee, T. Kim, M. K. Sang, N. K. Hong, S. H. Ahn, and K. Y. Suh, Nat. Mater. **11**, 795 (2012).
[8] M. L. Hammock, A. Chortos, B. C. Tee, J. B. Tok, and Z. Bao, Adv. Mater. **25**, 5997 (2013).
[9] T. Q. Trung and N. E. Lee, Adv. Mater. **28**, 4338 (2016).
[10] G. Schwartz, B. C. Tee, J. Mei, A. L. Appleton, D. H. Kim, H. Wang, and Z. Bao, Nat. Commun. **4**, 1859 (2013).
[11] Y. K. Chang and F. C. Hong, Nanotechnology **20**, 195302 (2009).
[12] J. M. Weisse, C. H. Lee, D. R. Kim, and X. Zheng, Nano Lett. **12**, 3339 (2012).
[13] Z. Li, P. Dharap, S. Nagarajaiah, E. V. Barrera, and J. D. Kim, Adv. Mater. **16**, 640 (2004).
[14] T. Yamada, Y. Hayamizu, Y. Yamamoto, Y. Yomogida, A. Izadinajafabadi, D. N. Futaba, and K. Hata, Nat. Nanotechnol. **6**, 296 (2011).
[15] B. Nie, X. Li, J. Shao, H. Tian, D. Wang, Q. Zhang, and B. Lu, ACS Appl. Mater. Interf. **9**, 40681 (2017).
[16] Y. A. Samad, Y. Li, S. M. Alhassan, and K. Liao, ACS Appl. Mater. Inter. **7**, 9195 (2015).
[17] J. Zhao, G. Wang, R. Yang, X. Lu, M. Cheng, C. He, G. Xie, J. Meng, D. Shi, and G. Zhang, ACS Nano **9**, 1622 (2015).
[18] X. Li, T. Yang, Y. Yang, J. Zhu, L. Li, F. E. Alam, X. Li, K. Wang, H. Cheng, and C. T. Lin, Adv. Funct. Mater. **26**, 1322 (2016).
[19] J. L. Tanner, D. Mousadakos, K. Giannakopoulos, E. Skotadis, and D. Tsoukalas, Nanotechnology **23**, 285501 (2012).
[20] N. M. Sangeetha, N. Decorde, B. Viallet, G. Viau, and L. Ressier, J. Phys. Chem. C **117**, 1935 (2013).
[21] M. Zheng, W. Li, M. Xu, N. Xu, P. Chen, M. Han, and B. Xie, Nanoscale **6**, 3930 (2014).
[22] X. Zhao, Y. Yu, D. Li, and D. Wen, AIP Adv. **5**, 127216 (2015).
[23] B. Xie, L. Liu, X. Peng, Y. Zhang, Q. Xu, M. Zheng, T. Takiya, and M. Han, J. Phys. Chem. C **115**, 16161 (2011).
[24] J. Wang, X. J. Chen, K. M. Liao, G. H. Wang, and M. Han, Nanoscale Res. Lett. **10**, 1021 (2015).
[25] B. Radha, A. A. Sagade, and G. U. Kulkarni, ACS Appl. Mater. Inter. **3**, 2173 (2011).
[26] M. Han, C. Xu, D. Zhu, L. Yang, J. Zhang, Y. Chen, K. Ding, F. Song, and G. Wang, Adv. Mater. **19**, 2979 (2007).
[27] Y. Gong, Y. Zhou, L. He, B. Xie, F. Song, M. Han, and G. Wang, Eur. Phys. J. D **67**, 87 (2013).
[28] J. Schmelzer, S. A. Brown, A. Wurl, M. Hyslop, and R. J. Blaikie, Phys. Rev. Lett. **88**, 226802 (2002).

DOI:10.1063/1674-0068/cjcp1812296